Structural Characterization of the ADAM 16 Disintegrin Loop Active Site†

Jeffrey W. Norris,* Melanie M. Tomczak,‡ Ann E. Oliver, Nelly M. Tsvetkova, John H. Crowe, Fern Tablin, and Richard Nuccitelli§

Center For Biostabilization, University of California, 1 Shields Avenue, Davis, California 95616

Received April 2, 2003; Revised Manuscript Received June 30, 2003

ABSTRACT: ADAM's have various roles in intercellular adhesion and are thought to function by binding integrins through a 13 amino acid motif called the disintegrin loop. *Xenopus laevis* sperm express the protein ADAM 16, and peptides with the sequence of its disintegrin loop cause downstream events in eggs that require a rise in intracellular calcium similar to that occurring at fertilization. We characterized the portion of the ADAM 16 disintegrin loop responsible for causing egg activation. A peptide based on the C-terminal half of the motif, which includes a known integrin-binding sequence, is a partial agonist of calcium release. A peptide with the N-terminal sequence of the motif activates eggs in a manner virtually identical to the full-length peptide but lacks a recognized integrin-binding sequence. None of these peptides alter the permeability or fluidity of liposomes made from membrane lipids of *X. laevis* eggs. This result reflects the fact that the peptides do not cause calcium to leak across the egg membrane and indirectly provides evidence that they act through a receptor on the egg surface. The infrared spectrum of the full-length peptide has a strong absorption peak corresponding to a β-turn. We predict this structure occurs at the N-terminal sequence MPKT. A rearranaged peptide lacking any turns fails to activate eggs. These results provide the first structural information about the active site of an ADAM disintegrin loop. We interpret these results in terms of active site sequences from other ADAM's and the role of integrins during fertilization.

The family of transmembrane glycoproteins designated ADAM's[1] consists of approximately 30 members related by their extracellular metalloproteinase and disintegrin-like domains (*1*, *2*). The extracellular portions of these proteins may contain cysteine-rich domains, EGF-like repeats or thrombospondin repeats, and viral fusion domains. The disintegrin-like domains of ADAM's have been implicated in several cell−cell interactions including those associated with myocyte fusion (*3*), the adhesion of sperm to eggs during mammalian fertilization (*4*), initiation of development in amphibian eggs (*5*), and lymphocyte adhesion (*6*).

Four ADAM's have been suggested to play a role in fertilization. ADAM's 1, 2, and 3 (fertilin α, fertilin β, and cyritestin) are expressed on mouse spermatozoa (*7*, *8*). The disintegrin domains of ADAM's 2 and 3 are involved in the binding of sperm to eggs (*8*, *9*), while ADAM 1 may be involved in fusion of the gametes (*10*). ADAM 16, which is expressed on *Xenopus laevis* sperm, has the capacity to initiate development of eggs from this species (*5*). This event is signaled by a rise in the concentration of intracellular, free calcium in the eggs that is both necessary and sufficient to initiate development. Calcium release is necessary for the activation of eggs from all species that have been studied in this regard (*11*−*14*).

The mechanism by which a sperm stimulates the release of calcium from the egg's intracellular stores has been an area of research that has recently seen a remarkable amount of progress. Currently, several models exist for how the sperm causes this release (*15*). ADAM 16 is only one candidate molecule involved in this process, and has been suggested to activate eggs by binding to an uncharacterized receptor in the egg membrane (*5*, *16*). ADAM 16 has several characteristics that might be expected of such a sperm ligand: it is selectively expressed in testes, antibodies to the disintegrin loop of the protein label the surface of sperm, and peptides with sequences from its disintegrin domain induce calcium release in eggs.

The disintegrin-like domains of ADAM's are related to the soluble disintegrins from snake venom. The disintegrins in snake venom are derived from several types of metalloproteinases by cleavage of the polypeptide chain (reviewed in *17*). PII metalloproteinases have a single disintegrin available for cleavage, located at the C-terminus of the metalloproteinase. The disulfide bond patterns (*18*, *19*) of these disintegrins have been shown by NMR (*20*−*22*) to provide structure to the active site, which is a flexible loop

† This work was supported by NIH Grants HD07131 (to J.W.N.), T32-GM07377-24 (to J.W.N.), HL57810 (to F.T. and J.H.C.), and HD19966 (to R.L.N.); DARPA Grants N66001-00-C-8048 and 003067 (to J.H.C. and F.T.); and NSF Grant DBI-9602226 (to J.W.N.).

* To whom correspondence should be addressed. Tel.: 530-297-4695. FAX: 530-297-4697. E-mail: jwnorris@ucdavis.edu.

‡ Current Address: Department of Biochemistry, Queen's University, Kingston, ON, Canada.

§ Current Address: Section of Molecular and Cellular Biology, University of California Davis, 1 Shields Ave., Davis, CA 95616.

[1] Abbreviations: ADAM, a disintegrin and a metalloproteinase; DPH, 1,6-diphenyl-1,3,5-hexatriene; DMF, *N*,*N*′-dimethyl formamide; DNTB, 5,5′-dithiobis(2-nitrobenzoic acid); EC_{50}, effective concentration for 50% response; EDTA, ethylenediaminetetraacetic acid; FTIR, Fourier Transform Infrared; HEPES, *N*-(2-hydroxyethyl)piperazine-*N*′-(2-ethanesulfonic acid); MLV, multilamellar vesicle; n_H, Hill coefficient; NMR, nuclear magnetic resonance; TES, 2-[(2-hydroxy-1,1-bis[hydroxymethyl]ethyl)amino]ethanesulfonic acid; TMA-DPH, (1-(4-trimethylammoniumphenyl)-6-1,3,5-hexatriene; ULV, unilamellar vesicle; SEM, standard error of the mean.

10.1021/bi034517+ CCC: $25.00
Published on Web 07/26/2003

known as the "disintegrin loop". This loop typically has an RGD tripeptide at its tip, which is the primary integrin binding site. PIII metalloproteinases bear a close structural similarity to ADAM's, as they include both disintegrin and cysteine-rich domains located toward the C-terminus of the metalloproteinase. The distribution of cysteines throughout the sequences of the disintegrin domains from both classes of proteins are highly conserved. The disintegrin loops of ADAM's and disintegrins derived from PIII metalloproteinases generally lack RGD tripeptides and contain an additional cysteine residue at the base of the loop. In the case of catrocollastatin C, a disintegrin derived from a PIII metalloproteinase, this additional cysteine residue has been found to form a bond with the first cysteine in the cysteine-rich domain (*23*). Therefore, the active sites in the ADAM disintegrin-like domains may have additional complexity compared to those from disintegrins derived from PII metaloproteinases. The amino acid sequences for many of these domains are known (www.uta.fi/~loiika), but neither the higher-order structure nor the structural requirements for activity understood (*2*). In the present study, we have probed the requirements for activity in one such domain.

We have characterized the active site of ADAM 16 necessary for egg activation, using a series of peptides that span the disintegrin loop. Peptides with the full-length sequence of the loop or its N-terminal half activate eggs, whereas a peptide with the C-terminal sequence of the loop is a partial agonist, at best. None of the peptides used in this study interact with liposomes made from frog egg lipids, which indirectly suggests that they act through a protein in the egg membrane. The infrared spectrum of the full-length, disintegrin loop peptide provides evidence that it frequently folds into a β-turn in solution; we predict this turn occurs in the N-terminal portion of the peptide. Evidence supporting this assignment arises from our observation that eliminating the turn by rearranging the peptide sequence results in a loss of function. The charge distribution of the MPKTE sequence and the probability of a β-turn at this location provide additional evidence that this sequence is similar to the RGD in disintegrins derived from PII metalloproteinases. However, extensive studies of integrins on eggs from several species, including *X. laevis*, raises the possibility that this sequence acts through an as yet uncharacterized receptor.

MATERIALS AND METHODS

Materials. Human chorionic gonadotropin, pregnant mare's serum gonadotropin, iodoacetamide, diethyl ether, methanol, chloroform, Sephadex G-50, Triton X-100, and DNTB were purchased from Sigma-Aldrich, St. Louis, MO. All peptides were obtained from Synpep, Dublin, CA. Carboxyfluorescein, DPH, and TMA-DPH were purchased from Molecular Probes, Eugene, OR.

Preparation of Gametes. Mature, wild-type or albino, *X. laevis* females were induced to ovulate by a two-stage procedure of injecting pregnant mare's serum gonadotropin followed by human chorionic gonadotropin (*24*). The jelly layers surrounding the eggs were removed prior to the experiments by incubation in F1 medium (41.25 mM NaCl, 1.75 mM KCl, 0.5 mM Na_2HPO_4, 2.5 mM HEPES, 0.25 mM $CaCl_2$, and 0.06 mM $MgCl_2$, pH 7.8), containing 0.3% β-mercaptoethanol and adjusted to pH 8.9. After two minutes in this solution, the eggs were thoroughly washed with normal F1 medium. Ten minutes after the wash any damaged eggs were discarded.

Preparation of Peptides. The peptides used for this study had the following sequences: full-length ADAM 16 disintegrin loop, RMPKTECDLAEYA; N-terminus, YRMPKTES; C-terminus, ECDLAEY; the anisotropy control peptide, Bpa-RMPATACDLAEYA; and the rearranged disintegrin loop peptide, PELMDCTAREYKA. Each was purified by HPLC to 95% or greater homogeneity, and the molecular weight was confirmed by mass spectroscopy. For some experiments, the full-length and ECDLAEY peptides were carboxymethylated by incubation with 2 M equiv of iodoacetamide in oxidation buffer (250 mM Tris and 1 mM EDTA, pH 8.5), for 30 min at room temperature, in the dark (*25*). The peptides were purified by precipitation with a 3:1 mixture of diethyl ether and methanol, followed by centrifugation to pellet the precipitate, which was then washed three times with diethyl ether. Typically, less than 1% of the cysteine residues were in the reduced form after reaction with iodoacetamide, as determined with DTNB (see below). All peptides were stored at -20 °C as lyophilized powders and dissolved in F1 medium, immediately prior to use. The concentrations of all peptide solutions were determined by absorption at 280 nm, using extinction coefficients calculated for each peptide using the ProtParam tool available at the ExPASy website (www.expasy.ch).

Activation Experiments. For each concentration of peptide tested, eight dejellied eggs were transferred to a round-bottomed well in a microtiter plate using a 10 μL micropipet with the tip cut to an opening of 2 mm. Each egg was transferred with 4 μL of F1 medium, and additional F1 medium was added such that the final volume after peptide addition would be 50 μL. After addition of the peptide, the eggs were placed in an 18 °C incubator for 90 min prior to scoring. Fomation of partial cleavage planes in the egg membrane, observed through a dissecting microscope, was used as the criterion for scoring the effect of the peptides. Each replicate of the experiment was performed on a different day with a mixed population of eggs from at least two females to reduce individual variation. Using Sigmaplot v. 5.0 (Jandel Scientific, San Rafael, CA), the data set for each peptide was fit with a nonlinear, third-order Hill Equation.

Preparation of Lipid from X. laevis Eggs for Leakage and Anisotropy. Plasma membranes of *X. laevis* eggs were purified by the method of Monneron and d'Alayer (*26*), as modified by Luria et al. (*27*). The light and heavy fractions were combined and the lipids extracted with three volumes of a 3:1 mixture of chloroform and methanol. In preparation for leakage experiments or fluorescence anisotropy, the lipids in chloroform layer were dried under a vacuum overnight to remove any trace chloroform. For leakage experiments, the lipids were hydrated at a concentration of 10 mg/mL by gentle mixing in CTE buffer (100 mM carboxyfluorescein, 10 mM TES, 0.1 mM EDTA, pH 7.4), under nitrogen gas. The resulting multilamellar vesicles (MLV's) were converted to unilamellar vesicles (ULV's) by passing the solution through a hand-held extruder (Avestin, Ottawa, Canada) (*28*). Free carboxyfluorescein was separated from the ULV's by passing them through a Sephadex G-50 column with TEN buffer (10 mM TES, 50 mM NaCl, 0.1 mM EDTA, pH 7.4) as the mobile carrier. For fluorescence anisotropy, the lipids

Table 1: Effects of ADAM 16 Peptides on Permeability and Fluidity of Frog Egg Liposomes[a]

peptide	% leak	r_{DPH}	$r_{TMA-DPH}$
F1 medium	1.7 ± 0.1 (6)	0.176 ± 0.007 (11)	0.196 ± 0.008 (6)
full-length	8.4 ± 0.3 (4)	0.168 ± 0.008 (5)	0.206 ± 0.006 (4)
N-terminal	8.2 ± 0.1 (4)	0.177 ± 0.008 (6)	0.212 ± 0.005 (6)
C-terminal	8.5 ± 0.6 (4)	0.168 ± 0.004 (3)	0.208 ± 0.009 (3)
Bpa-peptide		0.094 ± 0.012 (3)	0.125 ± 0.006 (3)

[a] The percentage of carboxyfluorescein leaked by ULV's (% Leak), the DPH anisotropy of MLV's (r_{DPH}), and the TMA-DPH anisotropy of MLV's ($r_{TMA-DPH}$) are shown for frog egg liposomes in the presence of peptides based on the sequence of the ADAM 16 disintegrin loop as specified in Materials and Methods. SEM's are shown for the number of trials indicated in parentheses.

were hydrated in TEN buffer at 2.5 mg/mL for experiments with DPH or 0.5 mg/mL for experiments with TMA-DPH. The resulting MLV's were labeled with DPH (2 mM in DMF) for 30 min at a 1:400 molar ratio of dye: lipid or TMA-DPH (2 mM in DMF) for 45 min at the same ratio.

Leakage Experiments. The time course of fluorescence leakage from liposomes loaded with carboxyfluorescein was measured with a luminescence spectrometer (LS-50b, Perkin-Elmer, Norwalk, CT) using excitation and emission wavelengths of 450 and 550 nm, respectively. All samples were observed in a quartz fluorimetry cell with a 40 μL nominal volume and an 8.5 mm path-length (Starna, Atascadero, CA). Liposomes were used at a concentration optimized to provide the maximum signal after lysis with Triton X-100. Prior to the addition of peptide, the fluorescence from 45 μL of liposomes was monitored for 100 s to determine the basal leak rate. Peptide or F1 medium was then added to the liposomes and rapidly mixed, without removing the cell from the beam. The concentration of peptide used in this experiment was limited to 0.3 mM, as higher concentrations resulted in greater than 10% quenching of the fluorescence from carboxyfluorescien. The molar ratio of peptide to lipid in these experiments was approximately 5:1, based on the amount of lipid extracted from the eggs. After monitoring the fluorescence for 800 s, the vesicles were lysed with 0.05% Triton X-100, final concentration, to determine the maximum fluorescence yield for the sample.

Steady State, Fluorescence Anisotropy. Steady-state anisotropies of DPH and TMA-DPH labeled MLV's were measured with an L-format luminescence spectrometer (LS-50b, Perkin-Elmer). The excitation and emission wavelengths were set to 360 and 430 nm, respectively. Samples were observed in 3.5 mL, methacrylate fluorimetry cells with 10 mm path lengths (Perfector Scientific, Atascadero, CA). Peptides were incubated with 45 μL of liposomes at a final concentration of 3.1 mM (20% F1 medium) for 15 min prior to measurements. Immediately prior to observation, the samples were diluted to 3 mL with TEN buffer. Four to nine measurements were averaged for each sample, and each sample was replicated multiple times as indicated in Table 1. In parallel with each peptide sample, the anisotropy of the dyes in the presence of 20% F1 medium was included as a negative control.

Determination of Free Cysteine in Peptides. The function of disintegrin loop peptides depends on the oxidation states of the cysteine residues in their sequences. Oxidation of cysteine by DTNB yields a product that absorbs at 412 nm (*29*). Peptides were diluted to 1 mM in F1 medium and exposed to air at room temperature. At intervals of 15 min, 10 nmol of peptide was taken from this stock solution, added to 110 μL of DTNB reaction buffer (180 μM DTNB, 100 mM NaH_2PO_4, pH 8.0), and incubated for 15 min at room temperature. The amount of free cysteine in each sample was determined from the absorption at 412 nm. With each trial, the absorbance at 280 nm was measured for a parallel sample prepared from the stock, as a control for possible peptide loss.

Infrared Spectroscopy. FTIR spectra were collected with a Perkin-Elmer, model 2000 FTIR spectrometer and recorded with the manufacturer's Spectrum 2000 software (Norwalk, CT). The sample compartment of the spectrometer was kept at 0% relative humidity by flushing it with dry air from a Whatman model 75−62 generator (Haverhill, MA). All measurements were made at room temperature (~23 °C). Samples were placed in a cell composed of two CaF_2 windows separated by a 6 μm thick Mylar spacer. Single beam spectra of both the buffer and sample were recorded in the same cell to ensure a constant path length. Two hundred and fifty-six scans, with a resolution of 4 cm^{-1}, were averaged for each sample. The difference between the sample and the buffer was calculated using the Spectrum software, and the water absorption at 2100 cm^{-1} was found to be flat. The amide I region of the spectrum was evaluated between 1620 and 1700 cm^{-1}, and no adjustment of the baseline was required prior to fitting. The spectra were exported to Sigmaplot v. 5.0 and Peak Fit v. 4.0 (Jandel Scientific, San Rafael, CA) for curve fitting. The spectra were fit as a sum of Pearson IV distributions having different wavenumbers and bandwidths. The secondary structure was then assigned to each distribution on the basis of peak wavenumber (*30*).

Prediction of Secondary Structure. The secondary structure of the disintegrin domain of ADAM 16 was predicted using the Chou−Fasman algorithm as implemented on the ExPASy website (*31*). Predictions for α-helicies were made using a seven amino acid window; whereas, five amino acid windows were used for predictions for β-sheets and turns. We used the amino acid propensities originally defined by Chou and Fasman, and each amino acid in the windows contributed equally to the prediction (*31*).

RESULTS

Effects of Peptides Derived from ADAM 16. We determined the percentage of *X. laevis* eggs activated by each of three peptides with sequences from the ADAM 16 disintegrin loop (Figure 1). Egg activation was evaluated by pigment contraction and the formation of partial cleavage planes in the plasma membranes of eggs. These phenomena are programmed, downstream effects that require calcium release but occur in response to sperm or any other stimuli capable of causing that release (*32*, *33*). Peptides were the reagents of choice in these experiments for two reasons: native ADAM's have not been purified and disintegrin loop peptides from ADAM's and disintegrins derived from PIII metalloproteinases mimic the corresponding recombinant proteins in functional assays (*4*, *34*−*39*).

The data sets for the peptides were compared after fitting them with a nonlinear, third-order Hill equation. The full-length peptide (RMPKTECDLAEYA) activated eggs in a

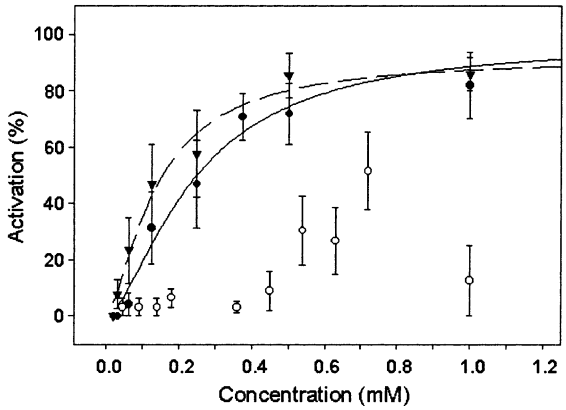

FIGURE 1: Dose response of eggs to peptides based on the sequence of the ADAM 16 disintegrin loop. We determined the responses of eggs to the full-length ADAM 16 peptide (closed triangles, $n = 4$), the N-terminal peptide (closed circles, $n = 4$), or the C-terminal peptide (open circles, $n = 8$). Error bars represent the SEM. The data for the full-length peptide (dashed line, $R^2 = 0.98$) and N-terminal peptide (solid line, $R^2 = 0.98$) were fit with 3rd order Hill Equations.

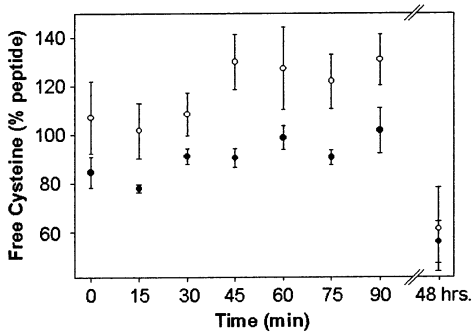

FIGURE 2: Oxidation of cysteine residues in peptides with the integrin binding sequence ECD. The full-length (open circles) and C-terminal (closed circles) peptides were resuspended in F1 medium (pH 7.8) at room temperature and exposed to room air to promote oxidation. The amount of free cysteine determined at the indicated intervals by Ellman's reaction. Error bars represent the SEM for $n = 3$.

dose-dependent manner with a Hill Coefficient (n_H) of 1.3 ± 0.2 and an effective concentration (EC_{50}) of 164 ± 16 μM. The N-terminal peptide (YRMPKTE), lacking the integrin recognition sequence ECD, activated eggs with a similar Hill coefficient $n_H = 1.6 \pm 0.3$, but at a higher effective concentration, $EC_{50} = 240 \pm 40$ μM ($p < 0.05$). Although the increased EC_{50} of the N-terminal peptide probably reflects the loss of structural constraints imposed by the C-terminal sequence, this result suggests that the N-terminal portion of the disintegrin loop is most likely responsible for the biological activity.

In agreement with this observation, we found that the C-terminal peptide (ECDLAEY) induced no response at any concentration in three of eight trials, and in the remaining five the response was nearly zero. The average response of eggs to this peptide was poorly fit by the nonlinear Hill Equation ($R^2 = 0.65$); so the C-terminal peptide is at best a partial agonist. This result is significant, because this peptide includes the integrin recognition sequence ECD. Thus, we tentatively suggest that the active site for these peptides acts independently of the ECD, a suggestion that we pursue further in th the next section.

Stability of the Integrin Recognition Sequence. Although the N-terminal portion of the disintegrin loop reproduces the effects of the entire loop, failure of the C-terminal peptide to elicit calcium release could be the result of cysteine residue oxidation in the integrin recognition sequence. Since carboxymethylation of disintegrin loop peptides based on ADAM 2 and Atrolysin A results in the loss of function (*36*, *37*, *39*), it has been suggested that the cysteine in the ECD sequence must be in the reduced state or participating in a disulfide bond for these peptide to have activity. In agreement with these observations, carboxymethylation of both the full-length and the C-terminal peptides completely blocked the capacity to activate eggs at concentrations as high as 1 mM. Carboxymethylation changes the charge and length of the cysteine side chain, which may, in turn, change the interaction of the peptides with their binding sites.

The question that follows is this: is the failure of the C-terminal peptide to induce the rise in intracellular calcium due to oxidation of the cysteine residues during its preparation and over the course of the experiment? We directly measured the rate at which the sulfhydryl group oxidized under the conditions used for our activation studies (Figure 2). After reacting with reduced cysteine residues, the oxidizing agent DNTB absorbs light at 412 nm. Absorption of tyrosine residues in both peptides was used to monitor the amount of peptide in each reaction. The ratio of these absorption values is proportional to the percentage of peptides with reduced cysteines. Immediately after resuspension, greater than 80% of both peptides were in the reduced state. We did not observe significant oxidation ($p < 0.05$ relative to $t = 0$) of the sulfhydryl group in these peptides until 48 h after resuspension. Thus, the failure of the C-terminal peptide to induce calcium release by eggs cannot be attributed to oxidation of the cysteine residue during the course of the experiment. We conclude that the ECD sequence is not likely to be involved in activation of the egg by the full-length peptide.

Nevertheless, there is a strong possibility that the cysteine residues are involved in maintaining structures and conformations within ADAM proteins. The cysteine in the ECD tripeptide is thought to provide an additional constraint on the disintegrin loops of ADAM's as compared to disintegrins derived from PII metalloproteinases (*4*, *23*, *36*, *38*). We will explore the role of conformation in the capacity of the full-length peptide to initiate calcium release by eggs in the final portion of this section.

Effects of Peptides Derived From ADAM 16 on Membrane Permeability. The fact that ADAM 16 peptides are based on a sperm protein does not ensure that they initiate a physiologically relevant calcium release. Disruption of the egg cortex could also lead to activation by causing a calcium leak. Peptides based on the ADAM 16 disintegrin loop induce calcium release by eggs in the absence of extracellular calcium (*5*). However, the close proximity of the cortical calcium-rich endoplasmic reticulum to the plasma membrane raises the possibility that membrane disruptive peptides could release sufficient calcium to activate an egg. Therefore, we evaluated the potentially destabilizing effects of these peptides using liposomes made from frog egg membrane lipids.

The capacity of the peptides to alter membrane permeability can be assessed by examining their effect on the leakage of carboxyfluorescein from ULV's. The dye is loaded at a self-quenching concentration and increases the

relative fluorescence intensity of the sample as it leaks into the medium (*40*). We report the net change in fluorescence observed in the 10 minutes following the addition of 0.25 mM peptide as the percentage of leakage for the full-length peptide, the C-terminal peptide, and the N-terminal peptide ADAM 16 peptides (Table 1). After correcting for the quenching of fluorescence by the peptides, it is apparent that they all cause increases in relative fluorescence intensity by approximately 6% relative to F1 buffer alone (1.8%). These apparent changes in permeability do not correlate with the capacity of the peptides to activate eggs.

Since membrane permeablilty is directly related to fluidity (*41*), we used fluorescence anisotropy to determine if the changes in permeability reflected by the leakage studies corresponded to changes in fluidity of the membrane bilayers. The polarizing dyes DPH and TMA-DPH are sensitive to changes in the order of the hydrocarbon core or the aqueous interface, respectively. None of the peptides significantly altered the anisotropy of either dye relative to the F1 buffer control (Table 1). Since we incubated the MLV's with approximately three times the saturating dose of peptide used in the egg-activation assay, it seems unlikely that these peptides affect the fluidity of membrane bilayers in the egg cortex at the doses used in those assays.

As a positive control for these experiments, we used a 14 amino acid peptide with the modified amino acid benzophenylalanine at the N-terminus (Bpa-RMPATACDLAEYA). The benzophenone group of this amino acid interacts with lipid bilayers and can be used to tether them to solid supports (*42*). This peptide could not be used as a positive control in the carboxyfluorescein experiments, because the benzophenone group quenches approximately 30% of the total fluorescence at 30 μM. However, the group neither polarizes light nor strongly interferes with emission by DPH or TMA-DPH. This peptide caused a 50% decrease in the anisotropy of DPH and a 25% decrease in the anisotropy of TMA-DPH relative to the F1 buffer (Table 1) (*43*, *44*). Such decreases in anisotropy correspond to increases in fluidity and permeability of the membrane lipids. The result provides evidence that a considerably more hydrophobic peptide than those derived from the ADAM 16 sequence is necessary to significantly alter membrane order.

Effects of Conformation of the Peptides on Activity. We expect that the conformations stabilized by the cysteine in ECD are functionally significant and frequently occur in biologically active peptides. However, structural data are difficult to obtain from peptides, because they are relatively unconstrained in solution. The integrin-binding sequence from fibronectin, GRGDS, forms a β-turn that is stable enough to be deduced by NMR (*45*, *46*). However, the time scale of chemical shifts in NMR spectroscopy ($\sim 10^3$ Hz) (*47*) is relatively slow compared to conformational changes in the peptide backbone. Therefore, we examined the structures that arise in the full-length disintegrin loop peptide of ADAM 16 by FTIR spectroscopy. This method has a fast time scale ($\sim 10^{12}$ Hz) (*47*) compared to the frequency of conformational changes of the peptide backbone ($\sim 10^9$ Hz) (*48*), making it ideal for studying the structures assumed by peptides in solution. Thus, a population of highly mobile peptides appears as a group of fixed conformations by FTIR that cannot be resolved by NMR. The carbonyl groups of peptide bonds absorb in the amide I region of the infrared spectrum (*49*), and different secondary structures are associated with different frequencies of absorption in this region (*50*−*53*).

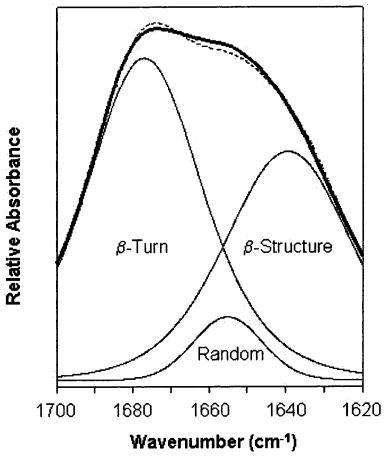

FIGURE 3: FTIR spectrum of the ADAM 16 disintegrin loop peptide. The calculated spectrum for the full-length peptide (dashed line) is the sum of three Pearson VI peaks (thin, solid lines) that fit the observed spectrum (bold, solid line) with $R^2 = 0.997$. Peak I is centered at 1677 cm^{-1} (54%) and corresponds to β-turns. Peak II is centered at 1655 cm^{-1} (7%) and corresponds to unordered structure. Peak III is centered at 1639 cm^{-1} (39%) and corresponds to a β-sheet or extended structure.

The FTIR spectrum of the full-length disintegrin loop peptide can be accurately fit by the sum of three distributions (Figure 3). The dominant peak at 1677 cm^{-1} represents 54% of the spectrum and corresponds to β-turn conformations. The remainder of the spectrum is described by two peaks at 1655 and 1639 cm^{-1}, which indicate the presence of unordered and extended structures, respectively. Since β-turn conformations generate such a large portion of the spectrum and are the only highly defined structure of the three, we hypothesized that it could be important for the peptide function. FTIR spectra lack positional information, and alternate methods are needed to determine the locations at which β-turns form in the ADAM disintegrin loop.

We used the Chou−Fasman algorithm to predict possible locations of β-turns in the ADAM 16 disintegrin-like domain. Within the disintegrin loop, the propensity for β-turn formation exceeds those for α-helix and β-sheet conformations only at the M and E residues in the N-terminal portion (Figure 4), indicating that turns can begin at these amino acids. The algorithm also stipulates that the probability of turn formation for the sequence of each proposed turn must exceed a minimum cutoff value based on known frequencies with which amino acids occur at different positions within a turn (*31*). Only the segment of the peptide with the sequence MPKT passes this second criterion for a stable β-turn (Table 2). As this algorithm was intended for the prediction of stable structures in crystallized proteins, we suggest that transient turns likely form at this location.

ADAM disintegrin loop peptides are sensitive to rearrangements that presumably disrupt their structure function relationships. We tested this hypothesis by rearranging the amino acids in the ADAM 16 disintegrin loop such that the propensity for β-turn formation was lower than that for α-helicies throughout the motif (Figure 5), and the MPKT sequence was lost in the process. The FTIR spectrum of this rearranged peptide (PELMDCTAREYKA) can be accurately

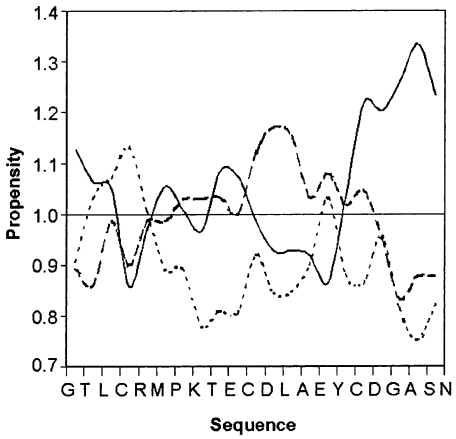

FIGURE 4: Conformation propensities for the ADAM 16 disintegrin loop. The Chou−Fasman algorithm, as implemented on the ExPASy server, was used to predict the propensities for β-turn (solid line), β-sheet (dotted line), and α-helical (dashed line) conformations in the disintegrin-like domain of ADAM 16. This figure shows the propensities for the integrin-binding motif, RMPKTECDLAEY, and several bracketing amino acids. The propensity for β-turn formation is greater than one and all other propensities at the M and E residues.

Table 2: Probabilities of Turn Formation for Tetrapeptides within the ADAM 16 Disintegrin Loop Sequence[a]

tetramer	p_{bend} ($\times 10^4$)
YRMP	0.08
RMPK	0.18
MPKT	1.16
PKTE	0.49
KTEC	0.58
TECD	0.49
ECDL	0.37
CDLA	0.34
DLAE	0.08
LAEY	0.45
AEYC	0.41
minimum	0.75

[a] The probability of turn formation (p_{bend}) is indicated for each four amino acid segment of the ADAM 16 disintegrin loop. The minimum probability for turn formation according to the algorithm is indicated in the last entry of the table.

fit by the sum of two distributions (Figure 6). The peak at 1680 cm^{-1} is associated with β-turns and represents only 18% of the total spectrum, which is considerably less than what we observed in the spectrum of the full-length peptide. This rearranged peptide has absolutely no capacity to induce the release of calcium in eggs at concentrations as high as 1 mM. These data provide evidence that a naturally occurring structure, which we suggest is a β-turn located at the sequence MPKT, is necessary for the function of the ADAM 16 disintegrin loop.

DISCUSSION

ADAM 16 is the only ADAM for which the disintegrin domain has been implicated in initiation of intracellular signaling. We have shown here that within the ADAM 16 disintegrin loop, the N-terminal sequence, RMPKTE, leads to downstream events requiring a rise in intracellular calcium. This sequence may represent another novel integrin-binding site within the ADAM family. Known binding sites include the following: (1) the tripeptide ECD in the disintegrin loop of ADAM 2 binds to the α6β1 integrin (*34*, *54*); (2) ADAM

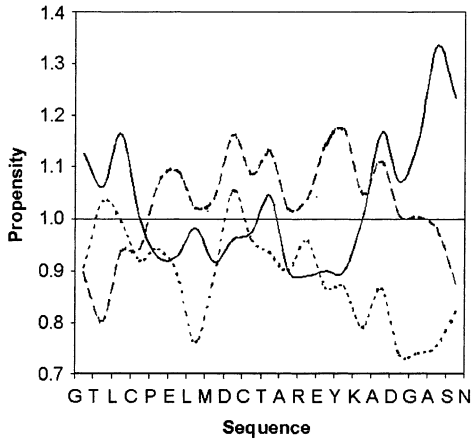

FIGURE 5: Conformational propensities resulting from rearranging the sequence of the ADAM 16 disintegrin loop. The integrin-binding motif of ADAM 16 was replaced with the sequence PELMDCT-AREYKA. The propensities for β-turn (solid line), β-sheet (dotted line), and α-helical (dashed line) conformations were determined for the resulting disintegrin-like domain. The α-helical conformation is greater than 1 and all other conformational propensities at all positions in the disintegrin loop region.

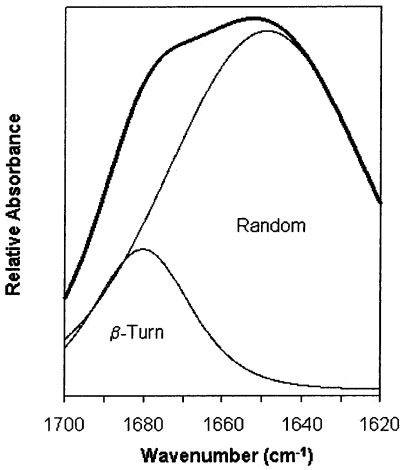

FIGURE 6: FTIR spectrum of the peptide with the rearranged sequence. The calculated spectrum (bold line) is the sum of two Pearson VI peaks (solid lines) that fit the observed spectrum with $R^2 = 0.9998$. The observed and calculated spectra overlap completely. Peak I is centered at 1680 cm^{-1} (18%) and corresponds to β-turns. Peak II is centered at 1649 cm^{-1} (82%) and corresponds to unordered structure.

28 binds the α4β1 integrin in lymphocytes through an extended charge surface on one face of the domain (*6*, *55*); (3) ADAM 1 has a putative binding site for integrins with the sequence DLEECDCG, which is outside the disintegrin loop motif (*56*); (4) hADAM 15, which is involved in tissue remodeling of athlerosclerotic lesions, binds the α9β1 integrin through an active site with the consensus sequence RX_6DLPEF within the disintegrin loop (*57*, *58*).

In addition to hADAM 15's ability to bind α9β1, it is the only ADAM that has an RGD tripeptide (*59*, *60*). This tripeptide is located in the X_6 portion of RX_6DLPEF and binds to the α$v\beta$3 integrin. The location of the RGD in hADAM 15 is in the same position of the disintegrin loop as the KTE in ADAM 16. We interpret this result as additional evidence that both halves of an ADAM disintegrin loop could serve as active sites nearly independently of each other.

Sequences homologous to RX_6DLPEF are present within all mammalian ADAM's, except ADAM's 10 and 17, and this motif has been implicated in gamete adhesion during fertilization (*57*). Disintegrin-like domains from hADAM15 and ADAM 2 expressed in bacteria, and then used in an in vitro fertilization assay, prevented the adhesion of mouse gametes. However, the recombinant disintegrin domain from ADAM 17, lacking the RX_6DLPEF motif, did not inhibit fertilization in the same type of assay. ADAM 16 also has this motif, but the majority of it, DLAEY, is in C-terminal half of the disintegrin loop, which lacks the capacity to initiate calcium release by eggs. Nevertheless, we cannot discount the possibility that this motif in the ADAM 16 disintegrin loop has the capacity to block the binding of *X. laevis* sperm to eggs.

The N-terminal half of the ADAM 16 disintegrin loop is the most likely portion of the sequence to fold into a β-turn, which is required for the biological effect. The KTE sequence within this domain was proposed to be an RGD homolog, because an ATA mutant of the N-terminal sequence failed to induce calcium release by eggs (*5*). In support of this hypothesis, peptides containing the sequence RGD have been observed to activate *X. laevis* eggs (*61*). Peptides with the sequence GRGDS also form highly stable Type II β-turns in solution (*46*). We suggest that the proline residue immediately preceding the KTE likely prompts the formation of this conformation in the ADAM 16 disintegrin loop. However, PKTE may not be a direct analogue of RGD, because RGE forms a different turn structure than RGD (*46*), fails to bind integrins, and does not activate eggs (*61*). These results reflect that the binding-site for the ADAM 16 disintegrin loop recognizes a weakly defined charge distribution, positive−neutral−negative, arranged in specific conformation.

Peptides with the RMPKTE sequence have previously been shown to cause calcium release by eggs in the absence of extracellular calcium (*5*), and we extend this observation by demonstrating that peptides based on the sequence of the ADAM 16 disintegrin loop do not release internal calcium stores by disrupting the egg membrane. Both observations indirectly suggest that the peptides act through a receptor on the egg surface. On the basis of apparent similarity of RMPKTE to RGD and its relationship to the location of the RGD in hADAM 15, it is tempting to speculate that $\alpha v\beta 3$ is the receptor involved. The αv subunit is the only integrin to be identified on amphibian eggs, but it was found on eggs from the salamander *Pluerodeles waltl* (*62*). Studies of eggs from a number of species, including *X. laevis*, raise the possibility that another, unidentified receptor may be involved, as we discuss below.

Integrins have been found on the surfaces of eggs from species as divergent as sea urchins and mice. In the eggs of the sea urchin *Strongylocentrotus purpuratus*, the $\alpha B\beta C$ integrin heterodimer has been identified (*63*). Upon fertilization, the vitelline envelope, a proteinaceous matrix surrounding the egg, visibly swells. The extracellular portion of $\alpha B\beta C$ remains associated with this matrix, suggesting a tight association between integrin and matrix. Since ADAM's have not been identified in this species, integrins may play a traditional role of adhering membrane to matrix.

In mice, studies of disintegrin loop peptides and disintegrin-like domains of ADAM 2 expressed in bacteria have provided compelling evidence that this protein can interact with the $\alpha 6\beta 1$ integrin on the surface of the egg (*34*, *54*, *64*). However, the necessity of this interaction is called into question by recent studies of eggs in which the genes for integrins have been knocked out. The integrins $\alpha 3\beta 1$, $\alpha 5\beta 1$, $\alpha 6\beta 1$, and $\alpha v\beta 3$ have been identified on the surfaces of mouse eggs by immunolocalization (*64*, *65*). Elimination of either the $\alpha 6$ (*66*) or $\beta 1$ (*67*) integin subunits does not adversely affect fertilization. Additional treatment with function blocking monoclonal antibodies against either the $\beta 3$ or αv subunits also fails to reduce fertilization rates. In contrast to the integrin knockout eggs, sperm from ADAM 2 knockout mice bind eggs much less efficiently than normal sperm (*9*). These results have been interpreted as indicative that integrins are not necessary for sperm-egg binding and fusion (*67*).

The presence of integrins on the surfaces of *X. laevis* eggs is far less clear than for mice and sea urchins. The cloning and expression patterns of mRNA's for the integrin subunits $\alpha 2$, $\alpha 3$, $\alpha 4$, $\alpha 5$, $\alpha 6$, αIIb, and αv have been studied in *X. laevis* (*68*−*70*). Precursor and mature forms of the $\alpha 5$ (*71*) and αv (*70*) proteins have been detected in lysates from fertilized eggs (stage 1 embryos). Likewise, mRNA's for the $\beta 1$, $\beta 2$, $\beta 3$, and $\beta 6$ subunits have been characterized (*72*), but so far only $\beta 1$ protein has been found in egg lysates (*73*). The actual expression patterns of integrins are more complex than reflected simply by their detection in egg lysates. Both immunolocalization (*73*) studies and analyses of biotinylated proteins (*74*) on the surfaces of *X. laevis* oocytes provide evidence that the $\beta 1$ subunit is internalized during the maturation of Stage VI oocytes to eggs and is absent from the egg plasma membrane. Since it has only been identified in complexes with $\beta 1$ as the fibronectin receptor (*75*, *76*), $\alpha 5$ is unlikely to be on the egg surface, and a β subunit to complement αv has not been identified on the egg surface. Only a few classes of integrins have been detected in *X. laevis* eggs, and they can be intermittently expressed on the membrane. Thus, it remains unclear whether integrins are present on the egg at fertilization. Although more integrins may be identified as the sequencing of genomes from *X. laevis* and *Xenopus tropicalis* continue, an alternative interpretation of our results is that ADAM 16 interacts with a binding site other than an integrin.

In summary, we have determined several characteristics that are necessary for the activation of *X. laevis* eggs by the disintegrin loop of ADAM 16. First, the sequence required to cause this effect is located primarily in the N-terminal half of the disintegrin loop and is distinct from other sequences in disintegrin loops associated with binding to integrins such as ECD and RX_6DLPEF. Second, this sequence is the most likely portion of the disintegrin loop to form a stable β-turn, which is necessary for the effects caused by the peptides described here. Third, the oxidation state of the cysteine residue in the disintegrin loop or its participation in a disulfide bond is not necessary for egg activation by the N-terminal sequence. Fourth, the peptides used in this study do not alter the permeability or fluidity of the plasma membrane, providing indirect evidence that they act through an as yet unidentified receptor on the egg surface.

ACKNOWLEDGMENT

The authors thank Diana G. Myles for helpful discussions and constructive criticism of this manuscript.

REFERENCES

1. Primakoff, P., and Myles, D. G. (2000) *Trends Genet. 16*, 83−7.
2. Evans, J. P. (2001) *Bioessays 23*, 628−39.
3. Yagami-Hiromasa, T., Sato, T., Kurisaki, T., Kamijo, K., Nabeshima, Y., and Fujisawa-Sehara, A. (1995) *Nature 377*, 652−6.
4. Myles, D. G., Kimmel, L. H., Blobel, C. P., White, J. M., and Primakoff, P. (1994) *Proc. Natl. Acad. Sci. U.S.A. 91*, 4195−8.
5. Shilling, F. M., Magie, C. R., and Nuccitelli, R. (1998) *Dev. Biol. 202*, 113−24.
6. Bridges, L. C., Tani, P. H., Hanson, K. R., Roberts, C. M., Judkins, M. B., and Bowditch, R. D. (2002) *J. Biol. Chem. 277*, 3784−92.
7. Primakoff, P., Hyatt, H., and Tredick-Kline, J. (1987) *J. Cell Biol. 104*, 141−9.
8. Yuan, R., Primakoff, P., and Myles, D. G. (1997) *J. Cell Biol. 137*, 105−12.
9. Cho, C., Bunch, D. O., Faure, J. E., Goulding, E. H., Eddy, E. M., Primakoff, P., and Myles, D. G. (1998) *Science 281*, 1857−9.
10. Blobel, C. P., Wolfsberg, T. G., Turck, C. W., Myles, D. G., Primakoff, P., and White, J. M. (1992) *Nature 356*, 248−52.
11. Whitaker, M. J., and Steinhardt, R. A. (1982) *Q. Rev. Biophys. 15*, 593−666.
12. Nuccitelli, R. (1991) *Curr. Top. Dev. Biol. 25*, 1−16.
13. Jaffe, L. F. (1983) *Dev. Biol. 99*, 265−76.
14. Stricker, S. A. (1999) *Dev. Biol. 211*, 157−76.
15. Runft, L. L., Jaffe, L. A., and Mehlmann, L. M. (2002) *Dev. Biol. 245*, 237−54.
16. Shilling, F. M., Kratzschmar, J., Cai, H., Weskamp, G., Gayko, U., Leibow, J., Myles, D. G., Nuccitelli, R., and Blobel, C. P. (1997) *Dev. Biol. 186*, 155−64.
17. Jia, L. G., Shimokawa, K., Bjarnason, J. B., and Fox, J. W. (1996) *Toxicon 34*, 1269−76.
18. McLane, M. A., Marcinkiewicz, C., Vijay-Kumar, S., Wierzbicka-Patynowski, I., and Niewiarowski, S. (1998) *Proc. Soc. Exp. Biol. Med. 219*, 109−19.
19. Calvete, J. J., Schrader, M., Raida, M., McLane, M. A., Romero, A., and Niewiarowski, S. (1997) *FEBS Lett. 416*, 197−202.
20. Atkinson, R. A., Saudek, V., and Pelton, J. T. (1994) *Int. J. Pept. Protein Res. 43*, 563−72.
21. Senn, H., and Klaus, W. (1993) *J. Mol. Biol. 232*, 907−25.
22. Smith, K. J., Jaseja, M., Lu, X., Williams, J. A., Hyde, E. I., and Trayer, I. P. (1996) *Int. J. Pept. Protein Res. 48*, 220−8.
23. Calvete, J. J., Moreno-Murciano, M. P., Sanz, L., Jurgens, M., Schrader, M., Raida, M., Benjamin, D. C., and Fox, J. W. (2000) *Protein Sci. 9*, 1365−73.
24. Hedrick, J. L., and Nishihara, T. (1991) *J. Electron Microsc. Tech. 17*, 319−35.
25. Deutcher, M. P. (1990) *Guide to Protein Purification*, Vol. 182, Academic Press, Inc., London.
26. Monneron, A., and d'Alayer, J. (1978) *J. Cell Biol. 77*, 211−31.
27. Luria, A., Vegelyte − Avery, V., Stith, B. J., Tsvetkova, N., Wolkers, W. F., Crowe, J. H., Tablin, F., and Nuccitelli, R. (2002) *Biochemistry 44*, 13189−97.
28. MacDonald, R. C., MacDonald, R. I., Menco, B. P., Takeshita, K., Subbarao, N. K., and Hu, L. R. (1991) *Biochim. Biophys. Acta 1061*, 297−303.
29. Boyne, A. F., and Ellman, G. L. (1972) *Anal. Biochem 46*, 639−53.
30. Tomczak, M. M., Hincha, D. K., Estrada, S. D., Wolkers, W. F., Crowe, L. M., Feeney, R. E., Tablin, F., and Crowe, J. H. (2002) *Biophys. J. 82*, 874−81.
31. Chou, P. Y., and Fasman, G. D. (1974) *Biochemistry 13*, 222−45.
32. Steinhardt, R. A., and Epel, D. (1974) *Proc. Natl. Acad. Sci U.S.A. 71*, 1915−9.
33. Steinhardt, R. A., Epel, D., Carroll, E. J., Jr., and Yanagimachi, R. (1974) *Nature 252*, 41−3.
34. Bigler, D., Takahashi, Y., Chen, M. S., Almeida, E. A., Osbourne, L., and White, J. M. (2000) *J. Biol. Chem. 275*, 11576−84.
35. Evans, J. P., Kopf, G. S., and Schultz, R. M. (1997) *Dev. Biol. 187*, 79−93.
36. Jia, L. G., Wang, X. M., Shannon, J. D., Bjarnason, J. B., and Fox, J. W. (1997) *J. Biol. Chem. 272*, 13094−102.
37. Pyluck, A., Yuan, R., Galligan, E. J., Primakoff, P., Myles, D. G., and Sampson, N. S. (1997) *Bioorg. Med. Chem. Lett. 7*, 1053−1058.
38. Evans, J. P., Schultz, R. M., and Kopf, G. S. (1995) *J. Cell Sci. 108*, 3267−78.
39. Gupta, S., Li, H., and Sampson, N. S. (2000) *Bioorg. Med. Chem. 8*, 723−9.
40. Weinstein, J. N., Ralston, E., Leserman, L. D., Klausner, R. D., Dragsten, P., Henkart, P., and Blumenthal, R. (1984) in *Liposome Technology* (Gregoriadis, G., Ed.) pp 183−204, CRC Press, Boca Raton, FL.
41. Lande, M. B., Donovan, J. M., and Zeidel, M. L. (1995) *J. Gen. Physiol. 106*, 67−84.
42. Shen, W. W., Boxer, S. G., Knoll, W., and Frank, C. W. (2001) *Biomacromolecules 2*, 70−79.
43. Shinitzky, M., and Inbar, M. (1974) *J. Mol. Biol. 85*, 603−15.
44. Shinitzky, M., and Barenholz, Y. (1974) *J. Biol. Chem. 249*, 2652−7.
45. Ruoslahti, E. (1996) *Annu. Rev. Cell. Dev. Biol. 12*, 697−715.
46. Johnson, W. C., Jr., Pagano, T. G., Basson, C. T., Madri, J. A., Gooley, P., and Armitage, I. M. (1993) *Biochemistry 32*, 268−73.
47. Lane, A. N., Hays, L. M., Tsvetkova, N., Feeney, R. E., Crowe, L. M., and Crowe, J. H. (2000) *Biophys. J. 78*, 3195−207.
48. Hille, B. (1992) *Ion Channels of Excitable Membranes*, 2nd ed., Sinauer Associates, Sutherland, MA.
49. Byler, D. M., and Susi, H. (1986) *Biopolymers 25*, 469−87.
50. Dong, A., Huang, P., and Caughey, W. S. (1990) *Biochemistry 29*, 3303−8.
51. Dong, A., Caughey, W. S., and Du Clos, T. W. (1994) *J. Biol. Chem. 269*, 6424−30.
52. Dong, A. C., Huang, P., and Caughey, W. S. (1992) *Biochemistry 31*, 182−9.
53. Prestrelski, S. J., Byler, D. M., and Liebman, M. N. (1991) *Biochemistry 30*, 133−43.
54. Chen, H., and Sampson, N. S. (1998) *Chem. Biol. 6*, 1−10.
55. Bridges, L. C., Hanson, K. R., Tani, P. H., Mather, T., and Bowditch, R. D. (2003) *Biochemistry 42*, 3734−41.
56. Wong, G. E., Zhu, X., Prater, C. E., Oh, E., and Evans, J. P. (2001) *J. Biol. Chem. 276*, 24937−45.
57. Eto, K., Huet, C., Tarui, T., Kupriyanov, S., Liu, H. Z., Puzon-McLaughlin, W., Zhang, X. P., Sheppard, D., Engvall, E., and Takada, Y. (2002) *J. Biol. Chem. 277*, 17804−10.
58. Eto, K., Puzon-McLaughlin, W., Sheppard, D., Sehara-Fujisawa, A., Zhang, X. P., and Takada, Y. (2000) *J. Biol. Chem. 275*, 34922−30.
59. Nath, D., Slocombe, P. M., Stephens, P. E., Warn, A., Hutchinson, G. R., Yamada, K. M., Docherty, A. J., and Murphy, G. (1999) *J. Cell Sci. 112*, 579−87.
60. Zhang, X. P., Kamata, T., Yokoyama, K., Puzon-McLaughlin, W., and Takada, Y. (1998) *J. Biol. Chem. 273*, 7345−50.
61. Iwao, Y., and Fujimura, T. (1996) *Dev. Biol. 177*, 558−67.
62. Alfandari, D., Whittaker, C. A., DeSimone, D. W., and Darribere, T. (1995) *Dev. Biol. 170*, 249−61.
63. Murray, G., Reed, C., Marsden, M., Rise, M., Wang, D., and Burke, R. D. (2000) *Dev. Biol. 227*, 633−47.
64. Almeida, E. A., Huovila, A. P., Sutherland, A. E., Stephens, L. E., Calarco, P. G., Shaw, L. M., Mercurio, A. M., Sonnenberg, A., Primakoff, P., Myles, D. G., and et al. (1995) *Cell 81*, 1095−104.
65. Tarone, G., Russo, M. A., Hirsch, E., Odorisio, T., Altruda, F., Silengo, L., and Siracusa, G. (1993) *Development 117*, 1369−75.
66. Miller, B. J., Georges-Labouesse, E., Primakoff, P., and Myles, D. G. (2000) *J. Cell Biol. 149*, 1289−96.
67. He, Z. Y., Brakebusch, C., Fassler, R., Kreidberg, J. A., Primakoff, P., and Myles, D. G. (2003) *Dev. Biol. 254*, 226−37.
68. Whittaker, C. A., and Desimone, D. W. (1998) *Ann. N.Y. Acad. Sci. 857*, 56−73.
69. Whittaker, C. A., and DeSimone, D. W. (1993) *Development 117*, 1239−49.
70. Joos, T. O., Reintsch, W. E., Brinker, A., Klein, C., and Hausen, P. (1998) *Int. J. Dev. Biol. 42*, 171−9.
71. Joos, T. O., Whittaker, C. A., Meng, F., DeSimone, D. W., Gnau, V., and Hausen, P. (1995) *Mech. Dev. 50*, 187−99.

72. Ransom, D. G., Hens, M. D., and DeSimone, D. W. (1993) *Dev. Biol. 160*, 265−75.
73. Gawantka, V., Ellinger-Ziegelbauer, H., and Hausen, P. (1992) *Development 115*, 595−605.
74. Muller, A. H., Gawantka, V., Ding, X., and Hausen, P. (1993) *Mech. Dev. 42*, 77−88.
75. Hemler, M. E., Huang, C., and Schwarz, L. (1987) *J. Biol. Chem. 262*, 3300−9.
76. Hemler, M. E., Crouse, C., Takada, Y., and Sonnenberg, A. (1988) *J. Biol. Chem. 263*, 7660−5.

BI034517+